COMMENTS

Comments are short papers which criticize or correct papers of other authors previously published in the **Physical Review.** *Each Comment should state clearly to which paper it refers and must be accompanied by a brief abstract. The same publication schedule as for regular articles is followed, and page proofs are sent to authors.*

Comment on ''Self-similarity and transport in the standard map''

G. Zumofen[1] and J. Klafter[2]
[1]*Physical Chemistry Laboratory, ETH-Zentrum, CH-8092 Zürich, Switzerland*
[2]*School of Chemistry, Tel-Aviv University, Tel-Aviv 69978, Israel*
(Received 25 August 1997; revised manuscript received 26 June 1998)

We show that the numerical results obtained by Benkadda *et al.* [Phys. Rev. E **55**, 4909 (1997)] for the escape-time distributions in the standard map are at variance with previously published results [Europhys. Lett. **25**, 565 (1994)]. We discuss these discrepancies in terms of the relationships between the mean-squared displacement, sticking-time, and escape-time distributions. We also report on numerical investigations of the standard map. [S1063-651X(99)07103-2]

PACS number(s): 05.45.−a, 47.52.+j

In a recent paper Benkadda, Kassibrakis, White, and Zaslavsky (BKWZ) [1] have analyzed anomalous transport behavior in the iterated standard map. Self-similar structures in phase space and characteristic exponents of the mean-squared displacement (MSD) of escape and Poincaré-recurrence times have been studied numerically. In their paper [1] BKWZ disagree with some of our earlier results [2].

In what follows we would like to compare the numerical results obtained in Ref. [1] with those of Ref. [2]. In particular, we discuss the numerically determined exponents in light of the relationships between the exponents of the MSD, of the sticking- and escape-time distributions. These relationships were derived in previous work cited in Ref. [1] and were also derived in Refs. [3–7]. We also present some more numerical results on the escape and sticking-time distributions in the standard map. We begin with the relationships between the exponents and adopt the notations of Ref. [1] for clarity. The standard map is defined by the mapping equations

$$p_{n+1}=p_n+K\sin x_n, \quad x_{n+1}=x_n+p_{n+1}. \tag{1}$$

According to Eqs. (1.2), (1.3), and (4.5) of [1], the MSD of p is

$$\langle p^2\rangle \sim t^{\mu}, \quad 1<\mu<2 \tag{2}$$

where the case of $x(\mathrm{mod}\,2\pi)$ is considered. The escape-time distribution given by Eq. (5.4) of [1] is

$$\psi_{\mathrm{esc}}(t)\sim 1/t^{\gamma_{\mathrm{esc}}}, \tag{3}$$

so that, using Eq. (5.5) of [1],

$$\mu=\gamma_{\mathrm{esc}}-2. \tag{4}$$

Correspondingly, an enhancement in the diffusion behavior is expected to occur for $\gamma_{\mathrm{esc}}>3$.

This finding contradicts our basic understanding of the enhanced diffusion phenomenon. Equations (1)–(3) indicate that the broader the escape-time distribution is the less enhanced the diffusion is. We consider the broadness of the probability densities as a measure of anomaly so that with increasing broadness (smaller exponents) the anomaly increases. We argue that as long as a trajectory has not escaped from resonance with an accelerator mode, the particle moves approximately laminarly in one direction, which gives rise to a flight-type behavior well described by Lévy flights. The *broader* the distribution of resonance periods is, the *broader* the distribution of the flight periods is. In other words, the smaller the exponent of the escape-time distribution, the larger the exponent of the MSD.

We continue by first briefly reviewing the basic ideas of the Lévy-walk picture within the continuous-time random walk (CTRW) approach. The trajectories are thought to be composed of random spatiotemporal increments. For Lévy walks the particles are supposed to move between turning points at a velocity chosen randomly from a given distribution and the temporal intervals are also chosen randomly according to a given distribution. The trajectory $r(t)$ therefore evolves as [3–7]

$$r(t)=r(t_i)+v_i(t-t_i), \quad t\in[t_i,t_{i+1}] \tag{5}$$

where i denotes the ith motion event. For the purpose of this paper we restrict the analysis to one dimension and to motion at a constant velocity v. v_i are thus velocities $v_i=\pm v$ with the sign chosen at random. The time t in Eq. (5) is restricted to the ith temporal interval $[t_i,t_{i+1}]$. The interval times $t_{i+1}-t_i$, termed waiting, trapping, or flight times [2–6], are considered to be random variables according to the power-law distribution

$$\psi(t)\sim t^{-\gamma}. \tag{6}$$

Within these assumptions the time evolution of the propagator $P(r,t)$, the probability of being at r at time t having started at the origin at time zero can be given in a closed form [2–6]. In Fourier $(r\to k)$–Laplace $(t\to u)$ space the propagator is

$$P(k,u)=\frac{\Psi(k,u)}{1-\psi(k,u)}, \tag{7}$$

where

$$\psi(k,u)=\mathcal{F}_{r\to k}\mathcal{L}_{t\to u}\delta(|r|-vt)\psi(t), \tag{8}$$

$$\Psi(k,u)=\mathcal{F}_{r\to k}\mathcal{L}_{t\to u}\delta(|r|-vt)\int_t^\infty \psi(t')dt'. \tag{9}$$

From the propagator the mean-squared displacement is calculated as

$$\langle r^2(t)\rangle=-\mathcal{L}^{-1}_{u\to t}\left(\frac{\partial^2}{\partial k^2}P(k,u)\right)_{k=0}. \tag{10}$$

Depending on the moments of $\psi(t)$ the diffusional motion is either regular or enhanced. We consider the case of a finite mean flight time, $\langle t_{\rm flight}\rangle<\infty$, which is relevant for Hamiltonian systems, and concentrate on the second moment. For a finite second moment, $\langle t^2_{\rm flight}\rangle<\infty$, the diffusion is regular while for a diverging second moment, $\langle t^2_{\rm flight}\rangle\vec{<}\infty$, the diffusion is enhanced. The asymptotic analysis of Eq. (10) yields the relationship between the exponent μ of the MSD and γ of the flight distribution [2–6],

$$\mu=\begin{cases}4-\gamma, & 2<\gamma<3\\ 1, & \gamma>3.\end{cases} \tag{11}$$

In order to apply the Lévy-walk approach to the standard map we consider the following correspondence. The trajectory $r(t)$ corresponds to $p_n=p(t)$. The flight times are specified by the sticking times, periods for which the trajectory is in resonance with an accelerating mode of motion. During such periods the trajectory $\mathbf{r}(t)=(p(t),x(t))$ is confined within the boundary layer Ω of the island system associated with an accelerating mode. Thus the sticking-time distribution can be given as

$$\psi_{\rm stick}(t)=\langle\delta[(\tau^{\rm out}-\tau^{\rm in})-t]\rangle, \tag{12}$$

where $\tau^{\rm in}$ and $\tau^{\rm out}$ are the times of entering and leaving the boundary layer Ω and the averaging is taken over the $[\tau^{\rm in},\tau^{\rm out}]$ realizations. In the study of Meiss, these periods correspond to the escape times of the *incoming set* [8]. Assuming that the behavior of the MSD is asymptotically dominated by these resonances, the flight times $[t_i,t_{i+1}]$ in Eq. (5) can be set to the sticking times and one may replace

$$\psi\leftarrow\psi_{\rm stick}\quad\text{and}\quad\gamma\leftarrow\gamma_{\rm stick}. \tag{13}$$

Consequently, the relationship between the exponent μ and $\gamma_{\rm stick}$ results from Eq. (11),

$$\mu=\begin{cases}4-\gamma_{\rm stick}, & 2<\gamma_{\rm stick}<3\\ 1, & \gamma_{\rm stick}>3.\end{cases} \tag{14}$$

No distinction is made between the sticking and escape times by BKWZ [1], so the corresponding exponents are considered to be the same. In Ref. [2] we have found that the two exponents differ by one. In order to provide evidence for the difference between the two exponents, we make use of the following arguments. Consistent with the definition of Ref. [1], the escape time $t_{\rm esc}(\mathbf{r}_0)$ denotes the time required for a trajectory, initiated at position $\mathbf{r}_0=(p_0,x_0)$ within the boundary layer Ω, to escape to the chaotic sea. Referring again to the work by Meiss, the escape times used here correspond to the escape times of the *accessible set* in Ref. [8]. The probability density of the escape times is

$$\psi_{\rm esc}(t)=\langle\delta[t-t_{\rm esc}(\mathbf{r}_0)]\rangle_{\mathbf{r}_0\in\Omega}, \tag{15}$$

where the average is taken over the boundary layer Ω. The initial coordinate $\mathbf{r}_0$ can be thought of as being the coordinate $\mathbf{r}(\tau)\in\Omega$ of a particular trajectory at time τ which has entered the boundary layer. Conversely, the coordinates of a trajectory during a sticking period $\mathbf{r}(\tau),\tau\in[\tau^{\rm in},\tau^{\rm out}]$, can be thought of as initial coordinates of trajectories to escape so that Eq. (15) can be written as

$$\begin{aligned}\psi_{\rm esc}(t)&=\langle\delta(t_{\rm esc}(\mathbf{r}(\tau))-t)\rangle_{\mathbf{r}\in\Omega}\\ &=\langle\delta(t_{\rm esc}(\mathbf{r}(\tau))-t)\rangle_{\tau\in[\tau^{\rm in},\tau^{\rm out}]},\end{aligned} \tag{16}$$

where the average in the last expression is taken over τ restricted to the sticking periods. Here we have taken into account that for conservative systems the invariant density is homogeneous in phase space. Equation (16) shows the equivalence between the averaging over the geometry and over the sticking periods associated with the boundary layer. We now assume a particular realization of a trajectory and denote by $[\tau_i^{\rm in},\tau_i^{\rm out}]$, $i=1,...,N$ its sticking intervals. For this trajectory the average in the second equality of Eq. (16) is cast into

$$\begin{aligned}\psi_{\rm esc}(t)&\simeq\frac{\Sigma_i^N\int_{\tau_i^{\rm in}}^{\tau_i^{\rm out}}\delta(t_{\rm esc}(\mathbf{r}(\tau))-t)d\tau}{\Sigma_i^N\int_{\tau_i^{\rm in}}^{\tau_i^{\rm out}}d\tau}\\ &=\frac{(1/N)\Sigma_i^N 1|_{(\tau_i^{\rm out}-\tau_i^{\rm in})>t}}{(1/N)\Sigma_i^N(\tau_i^{\rm out}-\tau_i^{\rm in})},\end{aligned} \tag{17}$$

where the sum in the numerator of the last expression is restricted to the cases where the interval time is larger than time t. Clearly, as $N\to\infty$, in the long trajectory limit, the numerator is the probability of finding an interval larger than t and the denominator is the average sticking time. Because $\tau^{\rm out}-\tau^{\rm in}=t_{\rm stick}$ the numerator and denominator of Eq. (17) can be calculated from $\psi_{\rm stick}$, resulting in

$$\psi_{\rm esc}(t)=\frac{1}{\langle t_{\rm stick}\rangle}\int_t^\infty\psi_{\rm stick}(t')dt', \tag{18}$$

where the denominator guarantees normalization. Thus

$$\gamma_{\rm stick}=\gamma_{\rm esc}+1. \tag{19}$$

This finding is compatible with the results in Ref. [8]. For the exponent μ of the MSD we obtain

$$\mu = 4 - \gamma_{\text{stick}} = 3 - \gamma_{\text{esc}}, \quad 1 < \gamma_{\text{esc}} < 2 \tag{20}$$

for enhanced diffusion with a diverging mean escape time. For $\gamma_{\text{esc}} > 2$ we expect a regular diffusion behavior with $\mu = 1$. Correspondingly, we also find

$$\langle |p| \rangle \sim \begin{cases} t^{1/\gamma_{\text{esc}}}, & 1 < \gamma_{\text{esc}} < 2 \\ t, & \gamma_{\text{esc}} > 2 \end{cases} \tag{21}$$

which follows from the length-time scaling relationship [5]. Obviously, Eq. (20) is at variance with Eq. (4). We note that the relevant quantity for the transport is ψ_{stick} while for the efficient numerical derivation of the asymptotic behavior ψ_{esc} is the quantity of choice because of its smaller exponent. For the Poincaré-recurrence times of trajectories initiated in the chaotic sea all traps have to be considered. We conclude that asymptotically the Poincaré-recurrence times are governed by the trap with the smallest γ_{stick}. We emphasize that $\gamma_{\text{stick}} > 2$ for all traps so that the mean Poincaré-recurrence time also remains finite in agreement with Kac's theorem [8].

The relationship between the exponents of escape and sticking times can be understood within the symbolic-dynamics formulation of the problem [9]. As mentioned above, the CTRW analysis is based on the distribution of time periods $t_{\text{flight}} \equiv t_{\text{stick}}$ of approximate laminar motion. During such periods the motion is either forward or backward. We now assume motion on a cylinder, $p \in [-\infty, \infty]$, $x \in [-\pi, \pi]$. Considering Eq. (1), we notice that forward motion, $p_{n+1} > p_n$, is associated with $x_n > 0$ and the analogously backward motion, $p_{n+1} < p_n$, is associated with $x_n < 0$. One can therefore partition the phase space into $x < 0$ associated with backward motion and into $x > 0$ associated with forward motion. Correspondingly, we introduce the letters L and R for positions of the trajectory in these two areas of the partitioned phase space.

Assuming that one single fundamental accelerating mode governs the asymptotic behavior of the motion so that an iteration step is accompanied by a forward or backward step of approximately one unit cell, the analysis of the motion in terms of CTRWs reduces to the analysis of the symbolic dynamics, namely, of sequences $LL \ldots LL$ and $RR \ldots RR$ composed of one letter. We associate the length of these sequences with the sticking times and find that the asymptotic behavior of the distribution of sticking times and of the lengths follow power laws with the same exponent. The numerical analysis can be based on one single trajectory by determining the sequences of either L or R letters. An alternative way is to determine the number of iterations required to reach the next RL letter combination for trajectories initiated at LR combinations, and vice versa, when L and R are interchanged.

To include the escape times in this picture we associate the escape time with the number of iterations required to reach the next RL combination for a trajectory initiated at any R, and to reach the next LR for initiation at any L. The probability density of these numbers of iterations is expected to follow the same asymptotic behavior as the probability density of the escape times. From this reasoning the relationship between sticking- and escape-time distributions in Eq. (18) is plausible.

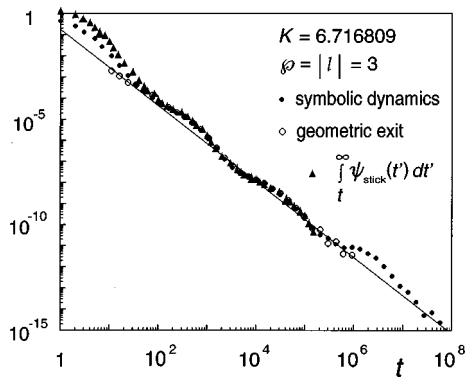

FIG. 1. Escape-time distributions obtained from the iterated standard map for the $K = 1.1 \times 2\pi$, $\wp = |l| = 3$ mode centered approximately at $p \simeq 0$, $x \simeq 2.0$. The escape times are given by dots for symbolic-dynamics calculations and by open circles for geometric exit conditions. Triangles are the results of the integration according to Eq. (18), as indicated. The full line gives a power law with the exponent equal to -1.8.

We have extended the numerical calculations, as outlined in Refs. [2,10], to longer time scales and have reproduced the values of the exponents we observed on a shorter time scale. For completeness we have also carried out the calculations for the value $K = 6.476\,939$ used in Ref. [1]. Here we present the results for three modes: the fundamental accelerating modes $\wp = |l| = 3$, $K = 1.1 \times 2\pi$ and $\wp = |l| = 5$, $K = 6.476\,939$, and the localizing mode $\wp = 2$, $|l| = 0$, $K = 6.476\,939$, where l denotes the number of unit cells stepped in period $\wp$. We calculated the sticking times from long trajectories by determining the intervals $[\tau^{\text{in}}, \tau^{\text{out}}]$ from the symbolic-dynamics criteria. In every case we checked that the symbolic-dynamics criteria were concerned with one particular accelerating or localizing mode, so that the resonance periods could unambiguously be assigned to that mode. The escape times were calculated for trajectories controlled in two ways. First, in the case of the symbolic dynamics the trajectories were initiated everywhere in the right half of a unit cell and the exit instances were determined according to the symbolic-dynamics criterion for the particular mode. Thus for resonance with a fundamental accelerating mode the criterion was given by motion in the forward direction in every step by one unit cell. For the localizing mode [10], the trajectory was initiated everywhere in the right half of the unit cell and the exit was determined from the condition of changing side in every step and of moving $l = +1$ and $l = -1$ in alternating steps. Second, the trajectories were initiated in a small domain enclosing the island structure and the exit was determined from leaving that domain.

In the numerical calculations the long trajectories used to determine the sticking times were of the order of 10^{11} iteration steps. We compared the histograms obtained from trajectories of different lengths with each other and changes were observed primarily in the outermost wings of the distributions. Therefore there is a scatter only for the data points of the longest times on the resolution of Figs. 1–3. We restricted the statistics of the sticking times to less than 10^6 number of steps because the trajectories of 10^{11} iteration

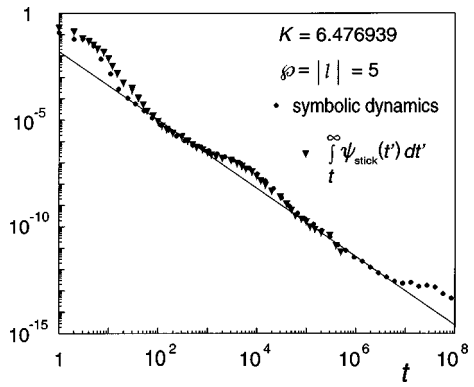

FIG. 2. Same as Fig. 1 but for the $K=6.476\,939$, $\wp=|l|=5$, mode centered approximately at $p\simeq 0$, $x\simeq 1.7$. Dots give the escape times calculated from symbolic dynamics and triangles are the results of the integration according to Eq. (18), as indicated. The full line gives a power law with the exponent equal to -1.6.

steps were too short for longer sticking times. In the case of escape times, trajectories of up to 10^8 iteration steps were used. For the symbolic-dynamics calculations a multigrid technique was applied by initiating the trajectories everywhere in the right half of a unit cell on a grid of $n\times n$ points excluding the area closely containing the stability islands. Within this area again trajectories were initiated on a grid of $n\times n$ points. The statistics were checked against an increasing grid resolution where the maximum was $n=2000$.

Our computed escape-time distributions are presented in Figs. 1–3. In Fig. 1, in addition to the symbolic-dynamics data, for $10<t<10^6$ the data obtained from geometrical exit conditions where the trajectories were initiated in the domain (p,x) corresponding to $[-0.25\pi,0.25\pi]\times[0.45\pi,0.8\pi]$ are plotted and the exit was determined from leaving this domain. In order to demonstrate the validity of Eq. (18), Figs. 1–3 also display the escape-time distributions calculated from $\psi_{\rm stick}$ according to Eq. (18), namely, $\langle t_{\rm stick}\rangle^{-1}\int_t^\infty \psi_{\rm stick}(t')dt'$. In the range of $10^2\leqslant t\leqslant 10^6$ the two decays are very similar; even the wiggly structures are convincingly reproduced. The overall decays follow approximately a power law with exponents $\gamma_{\rm esc}\simeq 1.8$, 1.6, 1.5 for the $\wp=|l|=3$, $\wp=|l|=5$, and $\wp=2$, $|l|=0$ modes, respectively. For $\wp=|l|=5$ the present value is in agreement with $\gamma_{\rm esc}$

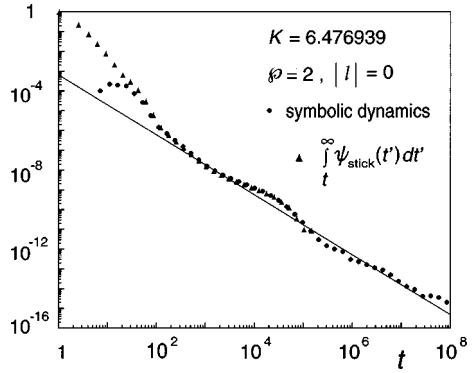

FIG. 3. Same as Fig. 1 but for the $K=6.476\,939$, $\wp=2$, $|l|=0$, mode centered approximately at $p\simeq\pi$, $x\simeq\pi/2$. Dots give the escape times calculated from symbolic dynamics and triangles are the results of the integration according to Eq. (18), as indicated. The full line gives a power law with the exponent equal to -1.5.

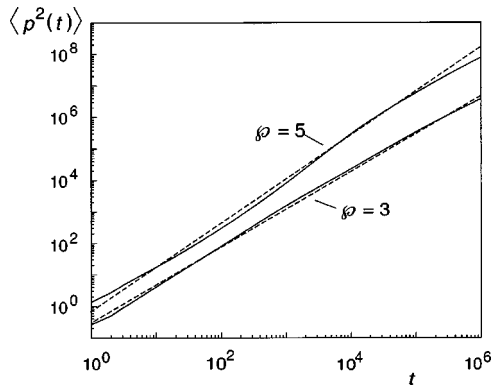

FIG. 4. The mean-squared displacement $\langle p^2(t)\rangle$ for $K=1.1\times 2\pi$ and 6.476 939 indicated by $\wp=3$ and 5. Simulation results are given by full lines. The dashed lines are power laws with exponents $\mu=1.2$ and 1.4 for $\wp=3$ and 5, respectively.

$\simeq 1.6$, found for the short time behavior by BKWZ; however, it is at variance with their value $\gamma_{\rm esc}=3.5$ determined for the long time behavior. For all three modes the decays show a characteristic oscillatory behavior. For $\wp=|l|=3$, $K=1.1\times 2\pi$ mode humps centered approximately at $t\simeq 3\times 10^2$, 2×10^4, and 3×10^6 and for the $\wp=|l|=5$, $K=6.476\,939$ mode humps centered at $t\simeq 7\times 10^3$ and 5×10^7 are observed. These oscillations can be compared with oscillations observed for transport properties in other hierarchical systems, for instance, for the autocorrelation function in ultrametric spaces [11] or on Sierpinski gaskets [12]. Correspondingly, the oscillations observed in the decay of the escape times are considered as an inherent property of the trajectories in the hierarchical structure of islands around islands. We therefore associate the three humps in Fig. 1 with the main island and with two generations of daughter islands and the two humps in Fig. 2 with the main island and with the first generation daughter islands. The agreement of the escape-time distributions obtained by the different methods may serve as a measure of the quality of the numerical data.

In Fig. 4 the MSD $\langle p^2(t)\rangle$ is shown for the two K values $1.1\times 2\pi$ and $K=6.476\,939$. The MSD was calculated from the same trajectories that were used to determine the sticking-time distributions. The simulation results are compared with power laws; the corresponding exponents are $\mu=1.2$ and 1.4, in agreement with $\mu=3-\gamma_{\rm esc}$, Eq. (20), using $\gamma_{\rm esc}=1.8$ and 1.6 given above for the accelerating modes. For $K=1.1\times 2\pi$ the value $\mu=1.2$ is somewhat smaller than the value $\mu=\frac{4}{3}$ determined on a shorter time scale, $t\leqslant 10^4$, in Ref. [13]. For $K=6.476\,939$ the exponent $\mu=1.6$ agrees reasonably with the value $\mu=1.62\pm 0.15$ observed by BKWZ. Oscillations are visible also for the MSD. For $\wp=5$ the first hump is observed approximately at $t\simeq 10^4$, in coincidence with the hump observed for the escape and sticking times in Fig. 2. Altogether, the simulation results indicate strongly that the exponent μ increases with decreasing exponent $\gamma_{\rm esc}$, in agreement with Eq. (20) but at variance with Eq. (4).

In conclusion, for two fundamental accelerating modes at different K values, and for one localizing mode, our numerical results indicate that $\gamma_{\rm stick}<3$. In the case of the accelerating modes, $\gamma_{\rm stick}<3$ is a necessary condition for the MSD to be enhanced according to the predictions of Eq. (14). Fur-

thermore, our data indicate very strongly that $\gamma_{\text{stick}} = \gamma_{\text{esc}} + 1$, in agreement with Eq. (19). Consequently, these data also indicate that the mean escape time diverges for all three modes. In the case of the accelerating modes, such a divergence is again a necessary condition for the MSD to be enhanced. Our numerical data deviate from those of BKWZ. For $K = 6.476\,939$ the exponent $\gamma_{\text{stick}} = 2.6$ of this work compares with 3.5 reported by BKWZ. Because we distinguish between t_{esc} and t_{stick} the exponent γ_{esc} of this work is smaller by approximately 1.9 than the value reported by BKWZ. The latter disagreement is regarded as resulting from conceptual differences in the approaches rather than from numerical inaccuracies. Our exponents γ_{stick} and μ are consistent with the relationship Eq. (14), which has been shown to be appropriate also in other systems [14,15]. Independent calculations carried our for the standard map and other systems are required in order to shed more light on these discrepancies.

We would like to thank Professor Meiss for private communications and Dr. M. F. Shlesinger for helpful discussions.

[1] S. Benkadda, S. Kassibrakis, R. B. White, and G. M. Zaslavsky, Phys. Rev. E **55**, 4909 (1997).
[2] G. Zumofen and J. Klafter, Europhys. Lett. **25**, 565 (1994).
[3] M. F. Shlesinger and J. Klafter, Phys. Rev. Lett. **54**, 2551 (1985).
[4] M. F. Shlesinger, B. J. West, and J. Klafter, Phys. Rev. Lett. **58**, 1100 (1987).
[5] G. Zumofen and J. Klafter, Phys. Rev. E **47**, 851 (1993).
[6] J. Klafter, M. F. Shlesinger, and G. Zumofen, Phys. Today **49**(2), 33 (1996).
[7] E. Barkai and J. Klafter, in *Chaos, Kinetics, and Non-linear Dynamics in Fluids and Plasmas*, edited by S. Benkadda and G. M. Zaslavsky (Springer, Berlin, 1988), p. 373.
[8] J. D. Meiss, Chaos **7**, 139 (1997).
[9] Hao Bai-lin, *Elementary Symbolic Dynamics and Chaos in Dissipative Systems* (World Scientific, Singapore, 1989).
[10] G. Zumofen and J. Klafter, Z. Naturforsch. A: Phys. Sci. **49**, 1141 (1994).
[11] M. Schreckenberg, Z. Phys. B **60**, 483 (1985).
[12] G. Zumofen, J. Klafter, and A. Blumen, Phys. Rev. A **44**, 8390 (1991).
[13] R. Ishizaki, T. Horita, T. Kobayashi, and H. Mori, Prog. Theor. Phys. **85**, 1013 (1991).
[14] T. Geisel, J. Nierwetberg, and A. Zacherl, Phys. Rev. Lett. **54**, 616 (1985).
[15] J. Klafter and G. Zumofen, Phys. Rev. E **49**, 4873 (1994).